ON THE SEARCH FOR TIGHT FRAMES OF LOW COHERENCE

XUEMEI CHEN[†], DOUGLAS P. HARDIN[*], AND EDWARD B. SAFF[*]

ABSTRACT. We introduce a projective Riesz s-kernel for the unit sphere $\mathbb{S}^{d-1}$ and investigate properties of N-point energy minimizing configurations for such a kernel. We show that these configurations, for s and N sufficiently large, form frames that are well-separated (have low coherence) and are nearly tight. Our results suggest an algorithm for computing well-separated tight frames which is illustrated with numerical examples.

1. INTRODUCTION

A set of vectors $X = \{x_i\}_{i\in I}$ is a *frame*[1] for a separable Hilbert space H if there exist $A, B > 0$ such that for every $x \in H$,

$$A\|x\|^2 \le \sum_{i\in I} |\langle x, x_i\rangle|^2 \le B\|x\|^2.$$

The constant A (B, resp.) is called the *lower (upper, resp.) frame bound*. When $A = B$, X is called a *tight frame*, which generalizes the concept of an orthonormal basis in the sense that the recovery formula $x = \frac{1}{A}\sum_{i\in I}\langle x, x_i\rangle x_i$ holds for every $x \in H$. For the finite dimensional space $H = \mathbb{H}^d$, where $\mathbb{H} = \mathbb{R}$ or $\mathbb{C}$, $X = \{x_i\}_{i=1}^N$ is a frame of $\mathbb{H}^d$ if and only if $\{x_i\}_{i=1}^N$ spans $\mathbb{H}^d$. We shall also use X to denote the matrix whose ith column is x_i and therefore we have

$$X \text{ is tight with frame bound } A \iff XX^* = AI_d,$$

where I_d is the $d \times d$ identity matrix.

Let $\mathcal{S}(d, N) := \{X = \{x_i\}_{i=1}^N \subset \mathbb{H}^d : \|x_i\| = 1\}$ be the collection of all N-point configurations on $\mathbb{S}^{d-1}$, the unit sphere of $\mathbb{H}^d$, where $\|\cdot\|$ denotes the ℓ_2 norm. If we have a unit norm tight frame $X \in \mathcal{S}(d, N)$, then it is well known that the frame bound

---

Date: September 20, 2020.

2010 *Mathematics Subject Classification.* Primary 42C15, 31C20 Secondary 42C40, 74G65.

Key words and phrases. frame, energy, tight, coherence, separation.

[†] The research of this author was supported by the U. S. National Science Foundation under grant DMS-1908880.

[*] The research of these authors was supported, in part, by the U. S. National Science Foundation under grant DMS-1516400.

[1]Depending on the context, we either consider X to be a multiset, allowing for repetition, or as an ordered list.

has to be N/d since

$$XX^* = \frac{N}{d} I_d. \tag{1.1}$$

Benedetto and Fickus show in [4] that frames that attain

$$\min_{X \in \mathcal{S}(d,N)} \sum_{i \neq j} |\langle x_i, x_j \rangle|^2 \tag{1.2}$$

are precisely the unit norm tight frames. We will call the function $|\langle x, y \rangle|^2$ the *frame potential kernel*. Ehler and Okoudjou [38] generalized this result to the p-frame potential kernel $|\langle x, y \rangle|^p$, see also [6] for recent results on p-frames.

Separation is a desirable property of a frame. It is quantified by the *coherence* $\xi(X)$ of a frame defined for $X \in \mathcal{S}(d, N)$ by

$$\xi(X) := \max_{i \neq j} |\langle x_i, x_j \rangle|.$$

The smaller the coherence, the better separated the frame is.

A straightforward method to find well-separated frames is to solve

$$\xi_N := \min_{X \in \mathcal{S}(d,N)} \xi(X) = \min_{X \in \mathcal{S}(d,N)} \max_{i \neq j} |\langle x_i, x_j \rangle|, \tag{1.3}$$

which has been studied in several works including Welch [68], Conway et al. [32], Strohmer and Heath [63], and more recently [41, 10]. The problem (1.3) is often referred as the *best line-packing* problem because it asks how to arrange N lines in $\mathbb{H}^d$ so that they are as far apart as possible. Conway et al [32] made extensive computations on this problem from a more general perspective: how to best pack n-dimensional subspaces in $\mathbb{R}^m$? There are also many other contributions using tools in geometry and combinatorics [35], and statistics [3]. A minimizer of (1.3) is called a *Grassmannian frame* by [63] and we shall use this terminology as well.

Our goal in this paper is to develop methods for generating tight frames with low coherence using energy minimization on the projective space $\mathbb{HP}^{d-1}$, which consists of all lines in $\mathbb{H}^d$ through the origin; namely, sets of the form

$$\ell(x) := \{\alpha x : \alpha \in \mathbb{H}\}, \tag{1.4}$$

for some $x \in \mathbb{S}^{d-1}$. We endow $\mathbb{HP}^{d-1}$ with the metric

$$\rho(\ell(x), \ell(y)) := \sqrt{2 - 2|\langle x, y \rangle|^2}, \qquad x, y \in \mathbb{S}^{d-1}, \tag{1.5}$$

which is the 'chordal' distance[2] and utilize kernels on $\mathbb{S}^{d-1} \times \mathbb{S}^{d-1}$ of the form:

$$K(x, y) = f\left(\rho(\ell(x), \ell(y))\right) = f\left(\sqrt{2 - 2|\langle x, y \rangle|^2}\right), \quad x, y \in \mathbb{S}^{d-1} \subset \mathbb{H}^d. \tag{1.6}$$

The energy of $X = X_N = \{x_1, \ldots, x_N\}$ with respect to the kernel K is given by

$$E_K(X_N) := \sum_{i \neq j} K(x_i, x_j). \tag{1.7}$$

[2]The chordal distance between the lines $\ell(x)$ and $\ell(y)$ is given by $\min\{\|x - uy\| : u \in \mathbb{H}, |u| = 1\}$.

One seeks the infimum of (1.7) over all possible N point configurations on $\mathbb{S}^{d-1}$. Assuming K is lower semi-continuous on $\mathbb{S}^{d-1}\times\mathbb{S}^{d-1}$ so the infimum is attained, we define the *N-point minimal energy of kernel K* as

$$\mathcal{E}_K(\mathbb{S}^{d-1},N) := \min_{X\in\mathcal{S}(d,N)} E_K(X). \tag{1.8}$$

An N-point configuration that achieves the minimum (1.8) will be denoted by $X_N^*(K,\mathbb{S}^{d-1})$ (or X_N^* when there is no ambiguity). So far the minimal energy and optimal configuration have been confined to the sphere and generalizes to any compact set A, and will be denoted as $\mathcal{E}_K(A,N), X_N^*(K,A)$ respectively. Note that the frame potential $|\langle x,y\rangle|^2$ is of the form (1.6) and that the energy minimizers are precisely the unit norm tight frames. However, in general for $N>d$, these minimizers may not consist of well-separated lines.

To achieve well separation of lines our approach is to first consider a class of kernels that are strongly repulsive and analyze the approximate tightness of their energy minimizers relative to their frame potential energy. Specifically, we introduce the *Riesz projective s-kernel*

$$G_s(x,y) := \begin{cases} \log\dfrac{1}{1-|\langle x,y\rangle|^2}, & s=0 \\ \dfrac{1}{(1-|\langle x,y\rangle|^2)^{s/2}}, & s>0 \end{cases} \tag{1.9}$$

for $x,y\in\mathbb{S}^{d-1}$ and seek solutions to the problem

$$\min_{X\in\mathcal{S}(d,N)} \sum_{i\neq j} G_s(x_i,x_j). \tag{1.10}$$

The kernel G_s is a modification of the classical *Riesz s-kernel* defined for x,y in a normed linear space $(V,\|\cdot\|)$ as

$$R_s(x,y) = \begin{cases} \log\dfrac{1}{\|x-y\|}, & s=0 \\ \dfrac{1}{\|x-y\|^s}, & s>0. \end{cases} \tag{1.11}$$

In fact, as we will show in (3.5), the projective Riesz s-kernel G_s can also be represented in terms of R_s for an appropriate subspace V of matrices with the Frobenius norm.

Notice that minimizers of (1.10) will avoid antipodal points since the energy in that case would be infinite. The connection between projective Riesz s-kernels and Riesz s-kernels is more immediate in the real case $\mathbb{R}^d$; since $\|x\pm y\|^2 = 2\pm 2\langle x,y\rangle$, we have

$$\frac{1}{(1-|\langle x,y\rangle|^2)^{s/2}} = \frac{2^s}{\|x-y\|^s\|x+y\|^s}.$$

Thus the projective Riesz kernel is just the Riesz kernel with the multiplicative factor $\|x+y\|^s$ to account for antipodal points.

A major focus of this paper is to exploit connections between G_s and R_s and reduce solving the projective Riesz s-kernel minimization problem (1.10) to solving

$$\min_{X\subset\mathcal{D},|X|=N}\sum_{i\neq j}R_s(x_i,x_j), \tag{1.12}$$

where we take $\mathcal{D}$ to be the projective space, but embedded in a higher dimensional real vector space (see Section 3.2). There are well established theorems available in the minimal energy literature for Riesz s-kernels (see e.g. [14]) and we shall review some of them in Section 2.

The projective Riesz s-kernel for $s<0$ defined by $G_s(x,y):=-(1-|\langle x,y\rangle|^2)^{-s/2}$ is also interesting. For such s we will be solving

$$\min_{X\in\mathcal{S}(d,N)}\sum_{i\neq j}-(1-|\langle x,y\rangle|^2)^{-s/2}\qquad\qquad(s<0). \tag{1.13}$$

This coincides with (1.2) when $s=-2$. This paper shall focus on the $s\geq 0$ case in the analysis, but our numerical experiments will include optimal configurations of (1.13).

The contributions of this paper are two-fold:

- Derive minimal energy results for the projective Riesz kernel. See Theorems 4.1, 5.1, and 5.4.
- Develop methods for constructing nearly tight and well-separated frames. See Theorems 6.3 and 6.4 and numerical results in Section 7.3.

2. Minimal Energy Background

In this section we will introduce some necessary background on minimizing discrete energy and its relation to the continuous energy.

The discrete minimal energy problem is known to be challenging, and we have very limited knowledge about the optimal configuration even for the classical Riesz kernel case (1.12) on the 2-dimensional sphere. The following theorem settles the case when points are on a circle of a real vector space for a large class of kernels that includes Riesz kernels.

Theorem 2.1 (Fejes-Tóth, [40]). *If $r>0$ and $f:(0,2r]\to\mathbb{R}$ is a non-increasing convex function defined at 0 by the (possibly infinite) value $\lim_{t\to 0^+}f(t)$, then any N equally spaced points on a circle of radius r (in $\mathbb{R}^m$) minimizes the discrete energy $E_K(X_N)$ for the kernel $K(x,y)=f(\|x-y\|)$. If in addition, f is strictly convex, then no other N-point configuration on this circle is optimal.*

Less is known regarding optimal configurations for (1.12) beyond $\mathbb{S}^1$. For optimality of configurations with particular cardinality N and dimension $d>1$, see [30] and [14]. On the other hand, many asymptotic results (as $N\to\infty$) for optimal configurations on the sphere as well as on $\mathbb{R}^d$ are known (for examples of recent results, see [7], [48]).

For a set of N points $X=\{x_i\}_{i=1}^N$, the *separation distance* of X is defined as

$$\delta(X):=\min_{i\neq j}\|x_i-x_j\|.$$

The *best-packing problem* is to find the N-point configuration on A that maximizes the separation distance:

$$\delta_N(A) = \max_{X\subset A,\,|X|=N} \delta(X) = \max_{X\subset A,\,|X|=N} \min_{i\neq j} \|x_i - x_j\|. \tag{2.1}$$

It is immediate, for example, that the best N-point packing of $\mathbb{S}^1 \subset \mathbb{R}^2$ consists of N equally spaced points on the circle.

When $s \to \infty$, the minimization problem with respect to the Riesz kernel $R_s(x, y)$

$$\min_{X\subset A,|X|=N} E_{R_s}(X)$$

turns into the best-packing problem (2.1); more precisely,

Theorem 2.2 ([14]). *If $N \geq 2$ and $A \subset \mathbb{R}^m$ is a compact set of cardinality at least N, then*

$$\lim_{s\to\infty} \mathcal{E}_{R_s}(A, N)^{1/s} = 1/\delta_N(A),$$

where R_s is the Riesz kernel defined in (1.11)*. Furthermore, if X_s is an optimal configuration that achieves $\mathcal{E}_{R_s}(A, N)$, then every cluster point as $s \to \infty$ of the set $\{X_s\}_{s>0}$ on A is an N-point best-packing configuration on A.*

This discrete minimal energy problem is related to a continuous energy problem as we next describe. Let $\mathcal{M}(A)$ be the set of probability measures supported on A. For a general kernel K, the *potential function* of a measure $\mu \in \mathcal{M}(A)$ with respect to K is defined as

$$U_K^\mu(x) := \int_A K(x, y)\, d\mu(y),$$

provided the integral exists as an extended real number. The energy of μ is defined as

$$I_K(\mu) := \int_A U_K^\mu(x)\, d\mu(x) = \iint_{A\times A} K(x, y)\, d\mu(x)d\mu(y),$$

and the *Wiener constant* is

$$W_K(A) := \inf_{\mu\in\mathcal{M}(A)} I_K(\mu). \tag{2.2}$$

Likewise this infimum can be achieved, and the probability measure that optimizes the above problem is called the *K-equilibrium measure*. The *K-capacity* of the set A is defined by

$$\mathrm{cap}_K(A) := \frac{1}{W_K(A)}.$$

A set A has zero capacity means that $W_K(A) = \infty$, which makes the problem (2.2) trivial since every probabilistic measure generates ∞ energy.

We now present a classical theorem connecting the discrete minimal energy problem to the continuous one. Before that we introduce the weak* limit of measures. A sequence of measures μ_n converges weak* to μ if for every continuous function f on A,

$$\lim_{n\to\infty} \int f d\mu_n = \int f d\mu.$$

We also define δ_x to be the point mass probability measure on the point x. Moreover, given a finite collection of points X, its *normalized counting measure* is defined as

$$\nu(X) = \frac{1}{|X|} \sum_{x \in X} \delta_x.$$

Theorem 2.3 ([29], [14, Theorem 4.2.2])**.** *If K is a lower semicontinuous and symmetric kernel on $A \times A$, where $A \subset \mathbb{R}^m$ is an infinite compact set, then*

$$\lim_{N \to \infty} \frac{\mathcal{E}_K(A, N)}{N^2} = W_K(A). \tag{2.3}$$

Moreover, every weak limit measure (as $N \to \infty$) of the sequence of normalized counting measures $\nu(X_N^*)$ is a K-equilibrium measure.*

The proof of Theorem 2.3 for the case of a Riesz kernel can also be found in the book by Landkof [56, Eq. (2.3.4)].

We now review two important facts concerning Riesz kernels.

Theorem 2.4 ([60], [13], [14])**.** *Let $A \subset \mathbb{R}^m$ be a compact infinite subset of an α-dimensional C^1-manifold with A of positive α-dimensional Hausdorff measure.*

1. *If $s \in [0, \alpha)$, then the R_s-equilibrium measure on A is unique. Moreover, if the potential function $U_{R_s}^{\mu}$ is constant on A, then μ is the R_s-equilibrium measure on A.*
2. *If $s \in [\alpha, \infty)$, then A has R_s-capacity zero. Moreover, if $X_N^*(R_s, A)$ denotes an R_s-energy optimal N-point configuration for $N \geq 2$, then the sequence of normalized counting measures $\nu(X_N^*(R_s, A))$ converges to the uniform measure (normalized Hausdorff measure) on A in the weak* sense as $N \to \infty$ (this is a special case of the so-called Poppy-seed bagel theorem).*

3. An overview of the problem on the sphere

3.1. **Projectively equivalent configurations.** Note that for a kernel K of the form (1.6), the energy $E_K(X)$, $X = \{x_i\}_{i=1}^N \in \mathcal{S}(d, N)$, is invariant under any of the following operations on X:

(3.1)
- (i) Apply a unitary operator (or orthogonal operator if $\mathbb{H} = \mathbb{R}$) on X as $\{Ux_i\}_{i=1}^N$;
- (ii) Change the sign of any x_i;
- (iii) Permute $x_1, \ldots, x_N$.

Any configuration Y obtained from X by applying these operations is said to be *projectively equivalent* to X. For example, $\{x_1, x_2, x_3, x_4\}$ is projectively equivalent to $\{Ux_4, Ux_2, -Ux_3, Ux_1\}$.

Theorem 5.1 below states that the configuration of equally spaced points on the half-circle,

$$X_N^{(h)} := \{e^{i \cdot 0}, e^{i\frac{\pi}{N}}, e^{i\frac{2\pi}{N}}, \ldots, e^{i\frac{(N-1)\pi}{N}}\} \subset \mathbb{R}^2, \tag{3.2}$$

is optimal for (1.8) for a certain class of kernels K.

3.2. **From sphere to the projective space.** The projective space $\mathbb{HP}^{d-1}$ can be embedded isometrically into the space of $d \times d$ Hermitian matrices, denoted by $\mathbb{HM}^h_{d\times d}$ as we next describe. Note that $\mathbb{HM}^h_{d\times d}$ is a real vector space for both $\mathbb{H} = \mathbb{R}$ and $\mathbb{H} = \mathbb{C}$ with inner product in $\mathbb{HM}^h_{d\times d}$ defined as $\langle M_1, M_2\rangle = \text{Trace}(M_1^* M_2)$. This inner product induces the Frobenius norm $\|M\| = \|M\|_F$ on $\mathbb{HM}^h_{d\times d}$. We further note that $\mathbb{HM}^h_{d\times d}$ with the Frobenius norm can be identified with the Euclidean space $\mathbb{R}^m$ where $m = (d^2+d)/2$ when $\mathbb{H} = \mathbb{R}$ and $m = d^2$ when $\mathbb{H} = \mathbb{C}$ (e.g., when $\mathbb{H} = \mathbb{R}$ and $M = (M_{i,j})$ we take any ordering of the m numbers $\sqrt{2}M_{i,j}$ for $i < j$ and $M_{i,j}$ for $i = j$).

Recalling (1.4), we define $\Psi : \mathbb{HP}^{d-1} \to \mathbb{HM}^h_{d\times d}$ as $\Psi(\ell(x)) := p_x$ with $p_x := xx^*$ and $x \in \mathbb{S}^{d-1}$. Clearly, Ψ is well defined (i.e., independent of the choice of the representative of the line). We denote the range of Ψ by $\mathcal{D}$; that is, $\mathcal{D} := \Psi(\mathbb{HP}^{d-1}) = \Phi(\mathbb{S}^{d-1})$ where $\Phi := \Psi \circ \ell$.

For $x, y \in \mathbb{S}^{d-1}$, the following well known equality (see, e.g. [31]) establishes that Ψ is an isometry:

$$\rho\left(\ell(x), \ell(y)\right)^2 = 2 - 2|\langle x, y\rangle|^2 = \|p_x - p_y\|_F^2 = \|\Phi(x) - \Phi(y)\|_F^2. \tag{3.3}$$

It is used, for example, in works on phase retrieval, see e.g. [22, 45]. For the reader's convenience we note that the middle equality in (3.3) follows using the cyclic property of the trace:

$$\|p_x - p_y\|_F^2 = 2 - \langle p_x, p_y\rangle - \langle p_y, p_x\rangle = 2 - \text{Trace}(y^* x x^* y) - \text{Trace}(x^* y y^* x) = 2 - 2|\langle x, y\rangle|^2,$$

from which we also get

$$\langle p_x, p_y\rangle = |\langle x, y\rangle|^2. \tag{3.4}$$

Note that (3.3) shows that Ψ is an isometric embedding of $\mathbb{HP}^{d-1}$ in $\mathbb{HM}^h_{d\times d}$, and so we identify $\mathbb{HP}^{d-1}$ with $\mathcal{D}$. We remark that $\mathcal{D}$ is a real analytic manifold whose dimension $\dim(\mathcal{D}) = \dim(\mathbb{HP}^{d-1})$ is $d-1$ in the case $\mathbb{H} = \mathbb{R}$ and $2d-2$ in the case $\mathbb{H} = \mathbb{C}$ (see [10] or [57]).

Now we are able to consider a kernel of the form $K(x,y) = f\left(\sqrt{2 - 2|\langle x, y\rangle|^2}\right)$ on $\mathbb{S}^{d-1} \times \mathbb{S}^{d-1}$ as a kernel $K(x,y) = \widetilde{K}(p_x, p_y) = f(\|p_x - p_y\|)$ on $\mathcal{D} \times \mathcal{D}$. Specifically the projective Riesz s-kernel (see (1.9)) can be reexpressed as

$$G_s(x,y) = \begin{cases} \log \dfrac{2}{\|p_x - p_y\|_F^2} = \log 2 + 2R_s(p_x, p_y), & s = 0 \\[2ex] \dfrac{2^{s/2}}{\|p_x - p_y\|_F^s} = 2^{s/2} R_s(p_x, p_y), & s > 0. \end{cases} \tag{3.5}$$

This allows us to reformulate the minimal projective energy problem in terms of the Riesz minimal energy problem on the set $\mathcal{D}$. This technique was also employed in [27]. In the next two sections we apply results of Section 2 for the problems

$$\min_{\mu \in \mathcal{M}(\mathcal{D})} I_{R_s}(\mu) \tag{3.6}$$

$$\min_{\{p_i\}_{i=1}^N \subset \mathcal{D}} \sum_{i \neq j} R_s(p_i, p_j). \tag{3.7}$$

Similarly, the Grassmannian problem (1.3) is equivalent to the best-packing problem (2.1) on the projective space, which is to maximize the smallest pairwise distance between all the lines (frame vectors). Let $P = \{p_i\}_{i=1}^N \subset \mathcal{D}$. For any point $p_i \in \mathcal{D}$, we can find $x_i \in \mathbb{S}^{d-1}$ such that $p_i = x_i x_i^*$. By (3.3),

$$\delta^2(P) = \min_{i \neq j} \|p_i - p_j\|^2 = \min_{i \neq j} (2 - 2|\langle x_i, x_j \rangle|) = 2 - 2 \max_{i \neq j} |\langle x_i, x_j \rangle| = 2 - 2\xi(X). \tag{3.8}$$

So

$$\delta_N^2(\mathcal{D}) = \max_{\{p_i\}_{i=1}^N \subset \mathcal{D}} \delta^2(P) = \max_{\{x_i\}_{i=1}^N \subset \mathbb{S}^{d-1}} (2 - 2\xi(X)) = 2 - 2\xi_N. \tag{3.9}$$

The last equality is from the definition (1.3).

For any Borel probability measure μ on the sphere, this embedding also induces the pushforward (probability) measure μ_{proj} on $\mathcal{D} \subset \mathbb{HM}_{d\times d}^h$. By definition of a pushforward measure,

$$\mu_{\text{proj}}(\mathcal{B}) := \mu(\Phi^{-1}(\mathcal{B}))), \quad \text{for Borel measurable } \mathcal{B} \subset \mathcal{D}. \tag{3.10}$$

We shall also write $\Phi(\mu)$ for μ_{proj}.

To better understand μ_{proj}, we further consider the symmetrization μ_{sym} of a measure $\mu \in \mathcal{M}(\mathbb{S}^{d-1})$ defined as

$$\mu_{\text{sym}}(B) = \begin{cases} \dfrac{\mu(B) + \mu(-B)}{2}, & \mathbb{H} = \mathbb{R} \\ \dfrac{1}{2\pi} \displaystyle\int_0^{2\pi} \mu(e^{i\theta} B) d\theta, & \mathbb{H} = \mathbb{C} \end{cases}, \tag{3.11}$$

for Borel measurable $B \subset \mathbb{S}^{d-1}$.

It is not difficult to show that $\mu_{\text{sym}} = \tilde{\mu}_{\text{sym}}$ if and only if the pullback measures $\mu \circ \ell^{-1}$ and $\tilde{\mu} \circ \ell^{-1}$ agree. The injectivity of Ψ then shows

$$\Phi(\mu) = \Phi(\tilde{\mu}) \Longleftrightarrow \mu_{\text{sym}} = \tilde{\mu}_{\text{sym}}. \tag{3.12}$$

Let σ_{d-1} be the uniform measure (normalized surface measure) on $\mathbb{S}^{d-1}$. Then $\Phi(\sigma_{d-1})$, the pushforward measure of σ_{d-1} under Φ, is the uniform measure on $\mathcal{D}$. In fact, $\Phi(\sigma_{d-1})$ is the Haar invariant measure induced by the unitary group (see [27, Section 4.2]).

4. Large N behavior of optimal configurations

We first focus on the continuous problem

$$\min_{\mu \in \mathcal{M}(\mathbb{S}^{d-1})} \iint_{\mathbb{S}^{d-1} \times \mathbb{S}^{d-1}} G_s(x, y) \, d\mu(x) d\mu(y), \tag{4.1}$$

The results are of independent interest, and will be used in Section 6.

For future reference, we set

$$I_s(\mu) := I_{R_s}(\mu) = \iint_{\mathcal{D}\times\mathcal{D}} R_s(x,y)\ d\mu(x)d\mu(y)$$

and

$$J_s(\mu) := I_{G_s}(\mu) = \iint_{\mathbb{S}^{d-1}\times\mathbb{S}^{d-1}} G_s(x,y)\ d\mu(x)d\mu(y).$$

As previously discussed, the projective space $\mathcal{D}$ embedded in $\mathbb{R}^m$ is a smooth (C^∞) compact manifold, so Theorem 2.4 applies with $A = \mathcal{D}$ and $\alpha = \dim(\mathcal{D})$.

Theorem 4.1. *For the projective Riesz kernel $G_s(x,y)$, the following properties hold.*

1. *If $0 \le s < \dim(\mathcal{D})$, then μ is a G_s-equilibrium measure on $\mathbb{S}^{d-1}$ if and only if its symmetrized measure $\mu_{\rm sym}$ is the normalized surface measure σ_{d-1} on $\mathbb{S}^{d-1}$.*
2. *If $s \ge \dim(\mathcal{D})$, then $\mathbb{S}^{d-1}$ has G_s-capacity 0.*
3. *Let $s \ge 0$ and let X_N^* be a G_s-optimal N-point configuration on $\mathbb{S}^{d-1}$ for $N \ge 2$. Then the sequence of normalized counting measures $\nu(\Phi(X_N^*))$ converges weak* to the uniform measure $\Phi(\sigma_{d-1})$ on $\mathcal{D}$ as $N \to \infty$.*

Proof. (1) When $s > 0$, by (3.5) and the definition of a pushforward measure,

$$U_{G_s}^{\mu}(x) = \int_{\mathbb{S}^{d-1}} G_s(x,y)\ d\mu(y) = \int_{\mathcal{D}} \frac{2^{2/s}}{\|p_x - p\|^s} d\mu_{\rm proj}(p) = \text{const}\cdot U_{R_s}^{\mu_{\rm proj}}(p_x). \tag{4.2}$$

A similar equality holds for the log case $s = 0$: $U_{G_s}^{\mu}(x) = \text{const} * U_{R_s}^{\mu_{\rm proj}}(p_x) + \text{const}$.

Thus for $s \ge 0$, the uniform measure σ_{d-1} produces a constant potential function with the kernel G_s, so $\Phi(\sigma_{d-1})$ also produces a constant potential function with the Riesz kernel R_s. By Theorem 2.4(1), $\Phi(\sigma_{d-1})$ must be the unique minimizer of (3.6).

On the other hand, similar to (4.2),

$$\begin{aligned} J_s(\mu) &= \int_{\mathbb{S}^{d-1}}\int_{\mathbb{S}^{d-1}} G_s(x,y)\ d\mu(x)d\mu(y) \\ &= \int_{\mathcal{D}}\int_{\mathcal{D}} \frac{2^{2/s}}{\|p-p'\|^s} d\mu_{\rm proj}(p)d\mu_{\rm proj}(p') = \text{const}\cdot I_s(\mu_{\rm proj}). \end{aligned} \tag{4.3}$$

Again a similar equality holds for the log case. This implies that μ is a minimizer of (4.1) if and only if $\Phi(\mu) = \mu_{\rm proj}$ is a minimizer of (3.6), which has to be $\Phi(\sigma_{d-1})$. By (3.12), this is equivalent to $\mu_{\rm sym} = (\sigma_{d-1})_{\rm sym} = \sigma_{d-1}$. This proves that μ is an equilibrium measure if and only if its symmetrized measure $\mu_{\rm sym}$ is σ_{d-1}.

(2) With the relation (4.3), this is a direct consequence of Theorem 2.4(2).

(3) For the discrete case, similar to (4.3), we have $E_{G_s}(X_N) = \text{const}\cdot E_{R_s}(\Phi(X_N)) + \text{const}$. So X_N^* be a G_s-optimal N-point configuration on $\mathbb{S}^{d-1}$ if and only if $\Phi(X_N^*)$ is an optimal configuration for the Riesz kernel R_s on $\mathcal{D}$.

By Theorem 2.3, we conclude that the normalized counting measure $\nu(\Phi(X_N^*))$ converges to the R_s-equilibrium measure on $\mathcal{D}$ in the weak* sense. As shown in part (1), this unique equilibrium measure is $\Phi(\sigma_{d-1})$, when $s \in [0, \dim(\mathcal{D}))$. When $s \ge \dim(\mathcal{D})$, by Theorem 2.4(2), we also have $\nu(\Phi(X_N^*))$ converges to $\Phi(\sigma_{d-1})$.

□

5. Discrete minimal energy problem

In this section we consider discrete extremal energy problems, for a general class of projective kernels of the form (1.6). Once again, the optimal configuration is an equivalent class in the sense of (3.1). Theorem 5.1 is for the 1-dimensional sphere in the real vector space while Theorem 5.4 is a general result over $\mathbb{H}$. Corollary 5.6 addresses the special projective Riesz kernel case (1.10).

Theorem 5.1. *If $f : (0, \sqrt{2}] \to \mathbb{R}$ is a non-increasing convex function defined at zero by the (possibly infinite) value $\lim_{t\to 0^+} f(t)$, then $X_N^{(h)}$ given in (3.2) is an optimal configuration on $\mathbb{RP}^1$ for the problem (1.8) where K is as in (1.6). If, in addition, f is strictly convex, then up to the equivalence relation in (3.1), no other N-point configuration is optimal.*

Proof. By (3.3), $K(x, y) = f(\|p_x - p_y\|)$, so we need to consider the minimal energy problem (1.8) with the kernel function to be $f(\|x-y\|)$ on the compact set $\mathcal{D} = \Phi(\mathbb{S}^1)$. The map $\Phi : \mathbb{S}^1 \to \mathbb{RM}^h_{2\times 2}$ is precisely

$$\Phi : (x, y) \to \begin{bmatrix} x^2 & xy \\ xy & y^2 \end{bmatrix}.$$

As mentioned at the beginning of Section 3.2, $\mathbb{RM}^h_{2\times 2}$ is identified with $\mathbb{R}^3$ using the mapping $\begin{bmatrix} x^2 & xy \\ xy & y^2 \end{bmatrix} \to (x^2, \sqrt{2}xy, y^2)$. This way, $\mathcal{D}$ is a circle in $\mathbb{R}^3$ with radius $1/\sqrt{2}$.

With $r = 1/\sqrt{2}$, the function f satisfies the assumptions of Theorem 2.1, so

$$\sum_{i\neq j} K(x_i, x_j) = \sum_{i\neq j} f(\|p_{x_i} - p_{x_j}\|)$$

is minimized if $p_{x_1}, p_{x_2}, \ldots, p_{x_N}$ are equally spaced on the circle $\mathcal{D}$. One can easily show that Φ maps equally spaced points on half $\mathbb{S}^1$ to equally spaced points on $\mathcal{D}$. So minimizers of (1.8) are precisely the equivalence class of equally spaced points on half of $\mathbb{S}^1$. □

Remark 5.2. It is well known that $\mathbb{RP}^{d-1}$ is a compact Riemannian manifold. However, $\mathbb{RP}^{d-1}$ is topologically equivalent to a sphere only when $d = 2$.

Remark 5.3. The frame potential kernel $|\langle x, y\rangle|^2$ can be written as $g(\sqrt{2 - 2|\langle x, y\rangle|^2})$, where $g(t) = 1 - t^2/2$ is not convex on $[0, \sqrt{2}]$. As a consequence, Theorem 5.1 cannot be applied to the frame potential kernel. The conclusion of Theorem 5.1 is however true, but there is no uniqueness (see [4]).

The discrete minimal energy problem for the Riesz s-kernel is in general very hard as mentioned previously. The situation is slightly better for kernels that are a function of absolute value of inner product, as we have the following general characterization when an *equiangular tight frame* (ETF) exists. A frame $X = \{x_i\}_{i=1}^N$ is *equiangular* if $\dfrac{|\langle x_i, x_j\rangle|}{\|x_i\|\|x_j\|}$ is a constant for all $i \neq j$. An ETF is a frame that is equiangular and tight.

For frames in $\mathcal{S}(d,N)$, a necessary condition for the existence of ETF is $N \le d(d+1)/2$ for $\mathbb{H}=\mathbb{R}$ and $N \le d^2$ for $\mathbb{H}=\mathbb{C}$. The coherence has the famous Welch bound

$$\xi(X) \ge \sqrt{\frac{N-d}{d(N-1)}}, \quad \text{for all } X \in \mathcal{S}(d,N), \tag{5.1}$$

and is achieved by ETFs. This can be easily derived from the relation (cf. [31])

$$N + N(N-1)\xi(X)^2 \ge \sum_{i,j=1}^{N} |\langle x_i, x_j\rangle|^2 = \|XX^* - \frac{N}{d} I_d\|_F^2 + \frac{N^2}{d} \ge \frac{N^2}{d}. \tag{5.2}$$

The Welch bound also coincides with the simplex bound of the chordal distance in [32]. We refer interested readers to [65] for more details and [42] for a table on existing ETFs. The second inequality in (5.2) also shows that the frame potential is minimized when the frame is tight.

The second theorem is for both the real and complex case.

Theorem 5.4. *Let $\tilde{f} : (0,2] \to \mathbb{R}$ be a strictly convex and decreasing function defined at $t=0$ by the (possibly infinite) value $\lim_{t\to 0^+} \tilde{f}(t)$, and $f : (0,\sqrt{2}] \to \mathbb{R}$ be a strictly convex and decreasing function defined at $t=0$ by the (possibly infinite) value $\lim_{t\to 0^+} f(t)$. If N and d are such that an ETF exists, then*

(i) *it is the unique optimal configuration of (1.8) for the kernel $\widetilde{K}(x,y) = \tilde{f}(2-2|\langle x,y\rangle|^2)$;*
(ii) *it is also the unique optimal configuration of (1.8) for the kernel $K(x,y) = f(\sqrt{2-2|\langle x,y\rangle|^2})$.*

Proof. (i) From (3.3), $\widetilde{K}(x,y) = \tilde{f}(\|p_x - p_y\|^2)$. Let $X = \{x_1, x_2, \dots, x_N\}$ be an arbitrary configuration on the sphere and set $P_i := p_{x_i} = x_i x_i^*$. Then, by (3.4),

$$\begin{aligned} J :&= \sum_{i\ne j} \|P_i - P_j\|^2 = \sum_{i=1}^{N}\sum_{j\ne i}(2 - 2\langle P_i, P_j\rangle) = \sum_{i=1}^{N}\left(2(N-1) - 2\sum_{j=1}^{N}\langle P_i, P_j\rangle + 2\right) \\ &= 2N^2 - 2\sum_{i,j=1}^{N} |\langle x_i, x_j\rangle|^2 \le 2N^2 - 2N^2/d, \end{aligned}$$

where the last inequality follows from (5.2). Thus,

$$\begin{aligned} E_{\widetilde{K}}(X) &= \frac{N(N-1)}{1}\cdot\frac{1}{N(N-1)}\sum_{i\ne j}\tilde{f}(\|P_i - P_j\|^2) \\ &\ge \frac{N(N-1)}{1}\tilde{f}\left(\sum_{i\ne j}\frac{1}{N(N-1)}\|P_i - P_j\|^2\right) = N(N-1)\tilde{f}\left(\frac{1}{N(N-1)}J\right) \\ &\ge N(N-1)\tilde{f}\left(\frac{2N^2 - 2N^2/d}{N(N-1)}\right) = N(N-1)\tilde{f}\left(\frac{2N(1-1/d)}{(N-1)}\right). \end{aligned} \tag{5.3}$$

The first inequality becomes equality if and only if $|\langle x_i, x_j\rangle|$ is constant for $i \neq j$; i.e., X is equiangular. The second inequality becomes equality if and only if X is a unit norm tight frame. Therefore, if an ETF exists for a given d and N, then this ETF is the unique $\widetilde{K}$-energy minimizer.

Part (ii) is a direct consequence of (i). Indeed, $f(\sqrt{2-2|\langle x,y\rangle|^2}) = g(2-2|\langle x,y\rangle|^2)$, where $g(t) = f(\sqrt{t})$. Since f is decreasing and convex, the same holds for g, to which we apply (i). □

Remark 5.5. Theorem 5.4 shows that an ETF is *universally optimal* (see [30, 31]) in the sense that it minimizes the energy for any potential that is a completely monotone function of distance squared in the projective space.

The assumption of Theorem 5.4 (part (i)) is weaker than that of Theorem 5.1 as reflected in the above proof. For example, Theorem 5.4 part (i) recovers Proposition 3.1 of [38] since $|\langle x,y\rangle|^p = f(1-|\langle x,y\rangle|^2)$ with $f(t) = (1-t)^{p/2}$. It is easy to verify that $f(t)$ is decreasing and convex on $[0,1]$ when $p > 2$. However $(1-t^2)^{p/2}$ is not convex, and therefore part (ii) cannot be used to recover Proposition 3.1 of [38]. We refer the interested reader to [24] for more results on p-frame potential.

Both Theorems 5.1 and 5.4 apply to the projective Riesz kernel since $\log 1/t$ and $1/t^s$ are strictly decreasing and strictly convex.

Corollary 5.6. *For the projective Riesz s-kernel minimization problem* (1.10) *when* $s \in [0,\infty)$,

(i) *the configuration* $X_N^{(h)}$ *defined in* (3.2) *is optimal for* $\mathbb{S}^1 \subset \mathbb{R}^2$;
(ii) *if it exists, an ETF is the optimal configuration for* $\mathbb{S}^{d-1} \subset \mathbb{H}^d$.

Remark 5.7. The conclusions of Corollary 5.6 hold for $s = \infty$ (best line-packing problem). These results were mentioned in [63] and are also implied by Theorem 6.1.

In particular, the optimal configuration of $N = d+1$ points that solves (1.10) is given by the vertices of a regular d-simplex because it is an ETF. When $d = 3$, the results for ETF are well known for small values of N. We summarize these results in Table 1, where we also compare the optimal configurations of the projective Riesz kernel and the classical Riesz kernel. They only share the same optimal configuration for the $N = d+1$ case. Moreover, ETFs are optimal configurations for the projective kernel while nothing is known for the Riesz kernel in general.

We have explained intuitively why the projective Riesz kernels are better at promoting well-separated frames than the Riesz kernel. This is reflected in Table 1. For the first case $\mathbb{S}^1$ when $N = 4$, the optimal configuration for the projective Riesz kernel is two orthonormal bases with a 45 degree angle, which is a well-separated tight frame, while the optimal configuration for the Riesz kernel consists of 4 equally spaced points on $\mathbb{S}^1$. For the third row, an orthonormal basis is the optimal frame whereas 3 points on one great circle is not even a frame. For 6 points on a sphere, the Riesz optimal configuration is again two copies of the same orthonormal bases. More numerical support can be found in Section 7.

The Grassmannian frame consisting of 5 vectors is constructed by removing an arbitrary element of the optimal Grassmannian frame consisting of 6 vectors (ETF). The

TABLE 1. Optimal configuration comparison on $\mathbb{S}^{d-1} \subset \mathbb{R}^d$

	proj. Riesz kernel $s \in [0, \infty)$	Best line-packing $s = \infty$	Riesz kernel $s \in [0, \infty)$
$\mathbb{S}^1$, any N	equally spaced points on half circle		equally spaced points on $\mathbb{S}^1$
$\mathbb{S}^2, N = 2$	two orthogonal points		two antipodal points
$\mathbb{S}^2, N = 3$	any orthonormal basis		vertices of an equilateral triangle on a great circle
$\mathbb{S}^2, N = 4$	vertices of a regular tetrahedron (simplex)		
$\mathbb{S}^2, N = 5$	open, see Table 2	removing any vector from the 3×6 ETF, see [32, 5]	partially solved in [61]
$\mathbb{S}^2, N = 6$	3×6 ETF, or vertices of the icosahedron		octahedral vertices
$\mathbb{S}^{d-1}, N = d + 1$	vertices of the simplex		
$\mathbb{S}^{d-1}, N$	$d \times N$ ETF when exists		open

coherence of the Grassmannian frame (in both $N = 5$ and $N = 6$) is $1/\sqrt{5}$. We refer to [32] for more details.

It is not possible for 5 points to be an ETF in $\mathbb{R}^3$, and the optimal configuration of (1.10) remains open to the best knowledge of the authors. The numerical experiments in Table 2 indicate that optimal configurations have exactly 2 distinct inner products. These inner products depend on the value s. As $s \to \infty$, Theorem 6.1 below implies that the inner products converge to $1/\sqrt{5}$.

TABLE 2. Optimal configurations for projective Riesz kernel and best line packing when $N = 5, d = 3$.

	$s = 2$	$s = 10$	$s = 15$	$s = \infty$
$\{\lvert\langle x_i, x_j\rangle\rvert : i \neq j\}$	$\{0.293, 0.506\}$	$\{0.366, 0.478\}$	$\{0.389, 0.471\}$	$\{1/\sqrt{5} \approx 0.447\}$

We conjecture that if $X^* = \{x_1, x_2, x_3, x_4, x_5\}$ is an optimal configuration of (1.10) for $s \in [0, \infty)$ and $N = 5$, then the cardinality of the set $\{\lvert\langle x_i, x_j\rangle\rvert, i \neq j\}$ is 2. We remark that constructions of biangular tight frames are studied in [23].

6. Optimal configurations as frames

We show in this section that frames rising from (1.10) are well-separated and nearly tight asymptotically. Since the frame vectors will always be on the sphere, it is understood that $\mathcal{E}_{G_s}(N)$ refers to $\mathcal{E}_{G_s}(\mathbb{S}^{d-1}, N)$.

The following theorem is the analog of Theorem 2.2 for the projective Riesz s-kernel. It can be over the real or complex field.

Theorem 6.1. *The best line-packing problem is the limit of problem* (1.10) *as* $s \to \infty$*:*

$$\lim_{s\to\infty} \mathcal{E}_{G_s}(N)^{1/s} = \sqrt{\frac{1}{1 - \xi_N}}.$$

If, for $s > 0$*,* X_s *is an optimal configuration achieving* $\mathcal{E}_{G_s}(N)$*, then every cluster point as* $s \to \infty$ *of the set* $\{X_s\}_{s>0}$ *is a Grassmannian frame.*

Proof. By (3.5)

$$\mathcal{E}_{G_s}(N) = 2^{s/2}\mathcal{E}_{R_s}(\mathcal{D}, N)$$

Taking the sth root and letting $s \to \infty$, we have

$$\lim_{s\to\infty} \mathcal{E}_{G_s}(N)^{1/s} = \lim_{s\to\infty} \sqrt{2}\mathcal{E}_{R_s}(\mathcal{D}, N)^{1/s} = \frac{\sqrt{2}}{\delta_N(\mathcal{D})} = \sqrt{\frac{1}{1-\xi_N}}.$$

The last two equalities are from Theorem 2.2 and (3.9),

The second assertion is also a consequence of Theorem 2.2 since for any G_s-optimal configuration $\{x_i\} \subset \mathbb{S}^{d-1}$, the configuration $\{p_i = x_i x_i^*\}$ is R_s-optimal for $\mathcal{D}$. □

The Grassmannian frames have the best separation by definition, but Theorem 6.1 suggests that we are also able to find well-separated frames by solving (1.10) for large values of s. We will further show that projective Riesz energy minimizing frames are well-separated in the sense that their coherence have optimal order asymptotic growth (Theorem 6.3).

Let $B(x, r) \subset \mathbb{R}^m$ be the ball centered at x with radius r. For a number $\alpha > 0$ and a positive Borel measure μ supported on $A \subset \mathbb{R}^m$, we say that μ is *upper α-regular* if there is some finite constant C_A such that

$$\mu(B(x, r)) \le C_A r^\alpha \qquad \text{for all } x \in A,\ 0 < r \le \operatorname{diam}(A), \tag{6.1}$$

and similarly that μ is *lower α-regular* if there is some positive constant c_A such that

$$\mu(B(x, r)) \ge c_A r^\alpha \qquad \text{for all } x \in A,\ 0 < r \le \operatorname{diam}(A). \tag{6.2}$$

It is not difficult to verify that $\Phi(\sigma_{d-1})$, the uniform measure on $\mathcal{D}$, is both upper and lower $(\dim \mathcal{D})$-regular (see the Appendix).

We recall that $\delta_N(\mathcal{D})$ is the maximum of the separation distance among all possible N point configurations on $\mathcal{D}$. Since $\Phi(\sigma_{d-1})$ is lower $(\dim \mathcal{D})$-regular, there is a constant $C < \infty$ such that $\delta_N(\mathcal{D}) \le CN^{-\frac{1}{\dim \mathcal{D}}}$ for all N, which follows immediately by observing that the $\Phi(\sigma_{d-1})$ measure of an arbitrary packing in $\mathcal{D}$ is no more than $\Phi(\sigma_{d-1})(\mathcal{D}) = 1$. Expressing this bound in terms of coherence (recall (3.9)) gives

$$\xi_N \ge 1 - \frac{C^2}{2} N^{-\frac{2}{\dim \mathcal{D}}}. \tag{6.3}$$

The above bounds are attained by any sequence of best-packing configurations on $\mathcal{D}$ (e.g., see [14, Chapter 13]).

Based on the above observation, we say that a sequence (X_N) of N-point configurations in $\mathcal{D}$ is *well-separated* if there is some constant $\widetilde{C} > 0$ such that $\delta(X_N) \ge \widetilde{C} N^{-\frac{1}{\dim \mathcal{D}}}$ for all N. Equivalently, in terms of coherence, (X_N) is well-separated if

$$\xi(X_N) \le 1 - \frac{\widetilde{C}}{2} N^{-\frac{2}{\dim \mathcal{D}}}, \tag{6.4}$$

for all N.

We will show that the projective s-Riesz energy minimizing points are well-separated when $s > \dim \mathcal{D}$. This is a consequence of the following known theorem for optimal configurations on more general sets.

Theorem 6.2 ([50, Corollary 2]). *Suppose $A \subset \mathbb{R}^m$ is compact and supports an upper α-regular measure μ as in (6.1). Let $s > \alpha, N \geq 2$ be fixed. If X_N^* is an N-point minimizing configuration on A for the s-Riesz energy minimizing problem (1.12), then*

$$\delta(X_N^*) \geq C_1 N^{-\frac{1}{\alpha}}, \tag{6.5}$$

where $C_1 = \left(\frac{\mu(A)}{C_A}(1 - \frac{\alpha}{s})\right)^{1/\alpha} \left(\frac{\alpha}{s}\right)^{\frac{1}{s}}$.

We will next apply Theorem 6.2 to obtain the following bound on the coherence of optimal G_s configurations.

Theorem 6.3 (Separation). *Let $s > \dim \mathcal{D}$. If X_s is an N-point minimizing configuration of (1.10), then*

$$\xi(X_s) \leq 1 - \frac{C_2^2}{2} N^{-2/\dim \mathcal{D}}, \tag{6.6}$$

where the constant C_2 is independent of N and, in the case $\mathbb{H} = \mathbb{R}$, can be found in (6.8). Consequently, any sequence of such configurations is well-separated as $N \to \infty$.

Proof. By (3.5), if $X_s = \{x_i\}_{i=1}^N$ is an optimal configuration of (1.10), then $P_s = \{x_i x_i^T\}_{i=1}^N$ is an optimal configuration of (3.7). Appealing to Theorem 6.2 with $A = \mathcal{D}$, the projective space embedded in $\mathbb{HM}_{d\times d}^h$, and recalling that $\Phi(\sigma_{d-1})$ is upper $(\dim \mathcal{D})$-regular with constant $C_{\mathcal{D}} > 0$, we have

$$\delta(P_s) \geq C_2 N^{-\frac{1}{\dim \mathcal{D}}}, \tag{6.7}$$

where $C_2 := \left(\frac{1}{C_{\mathcal{D}}}(1 - \frac{\dim \mathcal{D}}{s})\right)^{\frac{1}{\dim \mathcal{D}}} \left(\frac{\dim \mathcal{D}}{s}\right)^{\frac{1}{s}}$. The inequality (6.6) then follows from (3.8).

In the case $\mathbb{H} = \mathbb{R}$, as shown in the Appendix (see (A.4)),

$$C_{\mathcal{D}} = \frac{2}{d-1}\gamma_d = \frac{2\Gamma(\frac{d}{2})}{(d-1)\Gamma(\frac{d-2}{2})\Gamma(1/2)},$$

where $\Gamma(\cdot)$ is the Gamma function. Therefore

$$C_2 = \frac{(d-1)(s-d+1)\Gamma(\frac{d-2}{2})\Gamma(1/2)}{2s\Gamma(\frac{d}{2})} \left(\frac{d-1}{s}\right)^{\frac{1}{s}}. \tag{6.8}$$

□

It is worth noting in the case $\mathbb{H} = \mathbb{R}$ that the expected coherence of an i.i.d. random frame $X \in \mathcal{S}(d, N)$ generated from the uniform distribution on the sphere satisfies $\mathbb{E}[\xi(X)] \approx 1 - C_d N^{-\frac{4}{d-1}}$ (see Appendix), which is significantly worse than optimal. This fact is also demonstrated numerically in Section 7 (see Figure 2).

We next show that the optimal configurations of (1.10) are nearly tight.

Theorem 6.4 (Nearly tight)**.** *Let $s \geq 0$. If $X_N = \{x_1, \ldots, x_N\} \in \mathcal{S}(d, N)$ is any optimal configuration for* (1.10) *for $N \geq 2$, then (treated as a matrix)*

$$\lim_{N\to\infty} \frac{1}{N} X_N X_N^* = \frac{1}{d} I_d. \tag{6.9}$$

Proof. Theorem 4.1(3) states that $\nu(\Phi(X_N)) = \dfrac{1}{N}\displaystyle\sum_{i=1}^{N} \delta_{\Phi(x_i)}$ converges weak* to $\Phi(\sigma_{d-1})$. Thus for every continuous function f defined on $\mathcal{D}$,

$$\lim_{N\to\infty} \int_{\mathcal{D}} f d\nu(\Phi(X_N)) = \int_{\mathcal{D}} f d\Phi(\sigma_{d-1}).$$

By the definition of a pushforward measure, this can be simplified to

$$\lim_{N\to\infty} \int_{\mathbb{S}^{d-1}} f \circ \Phi \; d\nu(X_N) = \int_{\mathbb{S}^{d-1}} f \circ \Phi \; d\sigma_{d-1};$$

that is,

$$\lim_{N\to\infty} \frac{1}{N} \sum_{i=1}^{N} f(\Phi(x_i)) = \int_{\mathbb{S}^{d-1}} f(\Phi(x)) d\sigma_{d-1}. \tag{6.10}$$

Let $f(\Phi(x)) = xx^*$ be a vector-valued function. Then (6.10) implies

$$\lim_{N\to\infty} \frac{1}{N} \sum_{i=1}^{N} x_i x_i^* = \int_{\mathbb{S}^{d-1}} xx^* d\sigma_{d-1}. \tag{6.11}$$

We need to integrate every entry of the right-hand side. Let $x = (x(1), x(2), \ldots, x(d))^T \in \mathbb{S}^{d-1}$, so that $xx^* = (x(i)\overline{x(j)})$. Then,

$$\text{if } i = j, \quad \int |x(j)|^2 d\sigma_{d-1} = \frac{1}{d} \int (|x(1)|^2 + \cdots + |x(d)|^2) d\sigma_{d-1} = \frac{1}{d};$$

$$\text{if } i \neq j, \quad \int x(i)\overline{x(j)} d\sigma_{d-1} = 0 \text{ by symmetry.}$$

Since $X_N X_N^* = \dfrac{1}{N}\displaystyle\sum_{i=1}^{N} x_i x_i^*$, from (6.11) we deduce that

$$\lim_{N\to\infty} \frac{1}{N} X_N X_N^* = \frac{1}{d} I_d.$$

□

Theorem 6.4 says that the optimal configurations are nearly tight asymptotically as $N \to \infty$ in relation to (1.1). More desirable would be a stronger result of the form

$$\left\| X_N X_N^* - \frac{N}{d} I_d \right\|_F = \mathcal{O}(N^{-q}), \quad q > 0. \tag{6.12}$$

The numerical experiments in Section 7 (left side of Figure 3) do indeed suggest a result like (6.12) holds at least for small values of s. The work [18] provides a partial explanation for this phenomenon. It studies the convergence rate of (6.10) for f in a

Sobolev space (which is the case for every entry of xx^*). The numerical experiments therein suggests that the s-Riesz minimizing configurations (when $s = 0, 1$) achieve the optimal order quasi Monte Carlo error bounds.

Regarding random tight frames, it is shown in [37, Corollary 3.21] that

$$\mathbb{E}\left(\left\|X_N X_N^* - \frac{N}{d} I_d\right\|_F^2\right) = N(1 - \frac{1}{d}),$$

which grows as N grows. Section 7 (right of Figure 3) shows that optimal configurations of (1.10) also outperforms random configurations on tightness.

7. numerical experiments

The numerical experiments conducted consider points in the real vector space, and were executed in Matlab. When solving (1.10) (or (1.13) for negative s), spherical coordinates are used so that the command `fminunc` (unconstrained minimization) can be employed. Four experiments were performed.

The first and the second experiments deal with the separation and tightness of the optimal configurations of (1.10) or (1.13), and are explained in Sections 7.1 and 7.2. Since the objective function has lots of local minima, in both experiments, we run `fminunc` with multiple random initializations to obtain a putative minimum. We then test whether the optimal configurations are nearly tight or have small coherence (well-separatedness).

The third experiment presents an algorithm for obtaining tight frames with good separation. As explained in Section 7.3, it is crucial to use a well-separated frame as an initialization.

7.1. **Good separation.** The first experiment explores the asymptotic behavior of the coherence $\xi(X) = \max_{i \neq j} |\langle x_i, x_j \rangle|$ of projective Riesz minimizing points for various values of s as N gets larger. The result displayed in Figure 1 is for $d = 3$ with points on $\mathbb{S}^2$. The number of points N ranges from 3 to 100. The separation result Theorem 6.3 only applies to $s > 2$, but our numerical experiment shows that the log case and $s = 1$ case are achieving smaller coherence. The $s = -2$ (frame potential) case has the worst behavior as its minimizers could contain repeated (or antipodal) points. Notice that the coherence gets smaller as s increases which is consistent with Theorem 6.1. Finally, the coherence curve was fit with $y = 1 - 3/N$, which reflects Theorem 6.3.

The second experiment computed the coherence of the projective Riesz minimizing points for $d = 6$ and relatively small values of N (from 6 to 40), as shown in Figure 2. Various s are computed and compared with the Welch bound (5.1), the Levenstein bound [58, 70]

$$\xi(X) \geq \sqrt{\frac{3N - d^2 - 2d}{(d+2)(N-d)}}, \quad \text{if } N > d(d+1)/2,$$

and the Sloane database http://neilsloane.com/grass/. The Sloane database has the best known line-packings or the smallest coherence given d, N, among which some are only putatively known. Figure 2 also includes uniform random configurations. For each

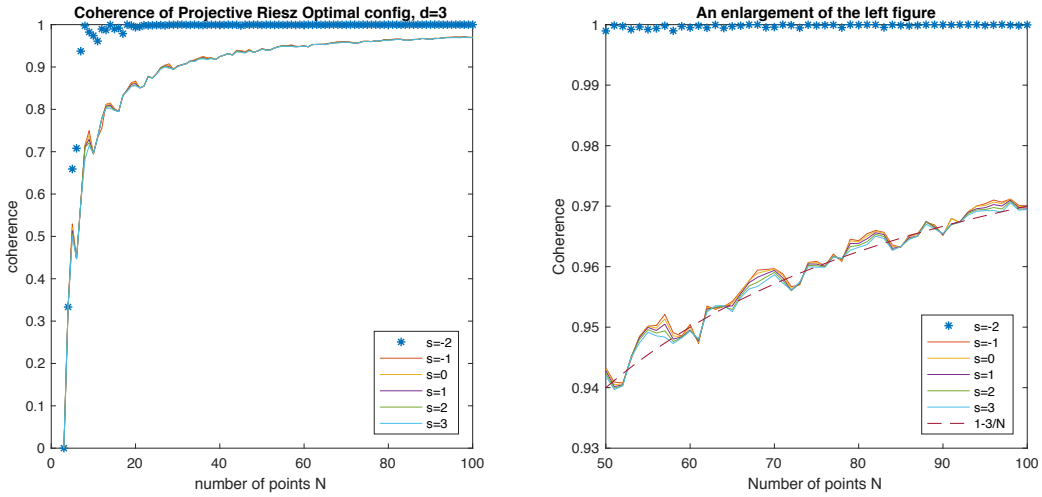

FIGURE 1

N, we display the coherence that is averaged over 20 samples. We again observe that larger s produces better separated frames, and $s = -2$ (frame potential case) produces highly correlated frames. For all values of s except for -2, (1.10) achieves the Welch bound when $N = 6, 7, 16$ (these are all the ETFs and thus universally optimal), and it achieves the Levenstein bound when $N = 36$. The 36 point configuration in $\mathbb{R}^6$ is the 6-dimensional lattice E_6 [41] and is also known to be universally optimal [31] although not an ETF. We further remark that our numerical experiments suggest that the Sloane grassmannian configurations for $d = 6$ and $N = 12$ and $N = 22$ may be universally optimal. This might also be anticipated from Figures 2 and 4. These figures might also suggest the universal optimality of the Sloane configuration for $N = 21$, however this turns out not to be the case.

7.2. **Nearly tight.** We addressed the tightness of the optimal configurations by computing $\|XX^T - \frac{N}{d} I_d\|_F$. We reuse the points generated from the first experiment with $d = 3$ and N ranging from 3 to 100. Figure 3 (left) shows the results for $s = -2, -1, 0, 1, 2, 3$. The $s = -2$ (frame potential) case recovers tight frames since by (5.2), Riesz (-2)-energy is equal to $\|XX^T - \frac{N}{d} I_d\|_F^2$ plus a constant. Unfortunately, the separation property deteriorates as s decreases while the tightness property improves. This is further validated by the poor tightness of the Sloane points as they correspond to the $s = \infty$ case. A least squares curve fitting was also performed for the peaks (least tight) for $s = 1$, which exhibits an $N^{-1/2}$ decay, a better rate than what Theorem 6.4 guarantees. Notice that the right side of Figure 3 also includes uniform random vectors for comparison. The randomly generated configurations exhibit worse behavior for both coherence and tightness. This has also been observed in [18].

The tightness for $d = 6$ with N ranging from 6 to 40 is illustrated in Figure 4 where the points generated from the second experiment are reused. The figure displays a clear pattern of improved tightness as s decreases.

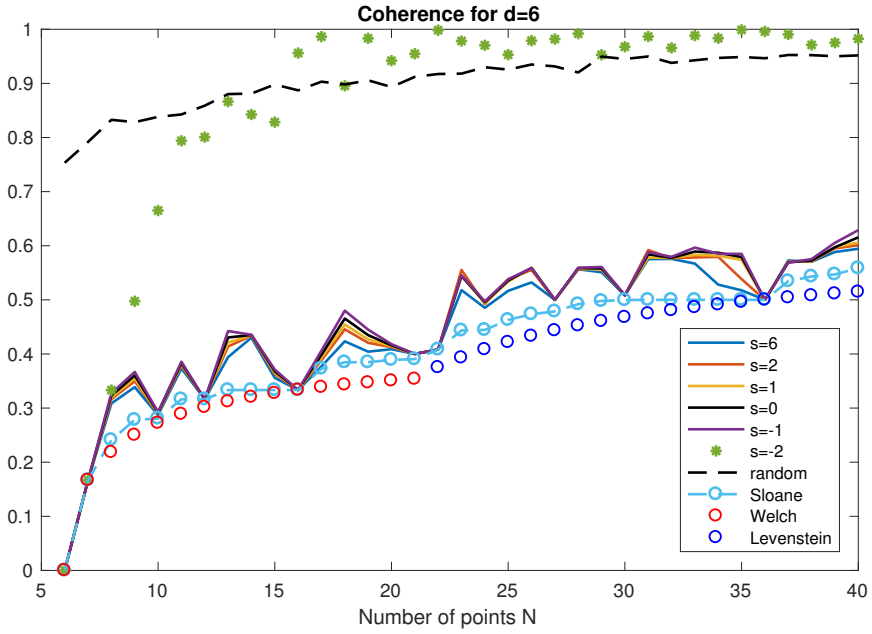

FIGURE 2

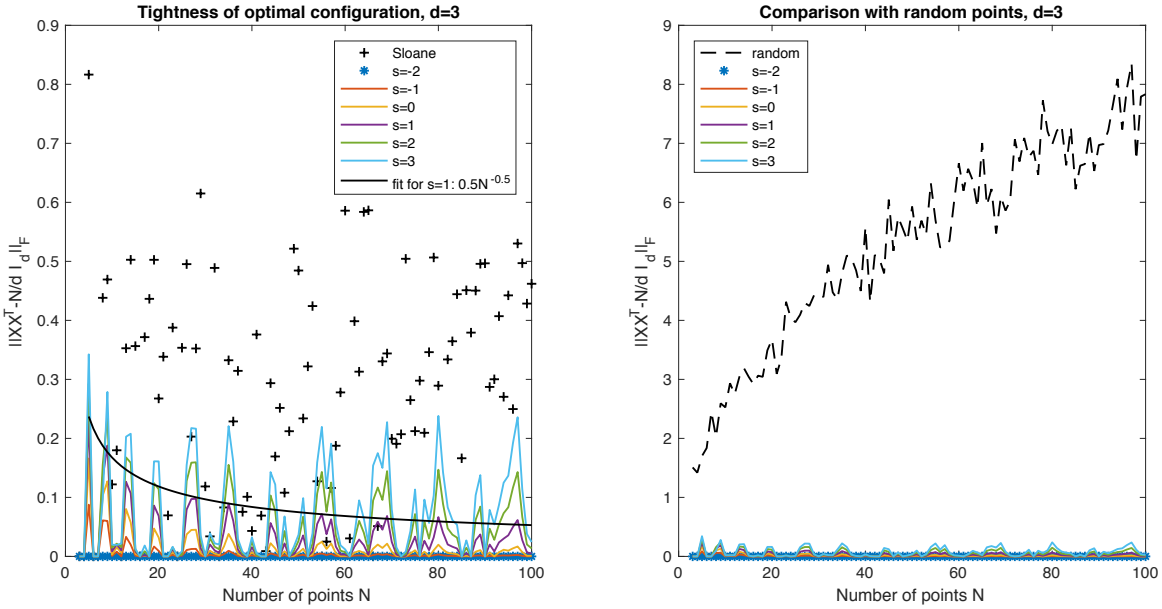

FIGURE 3. Tightness for $d = 3$. The right side plot includes random configurations.

7.3. **Achieving good separation and exact tightness.** In this section we present experiments based on a simple algorithm for obtaining frames with good separation and exact tightness. For the frame potential minimization problem ($s = -2$ of (1.13)),

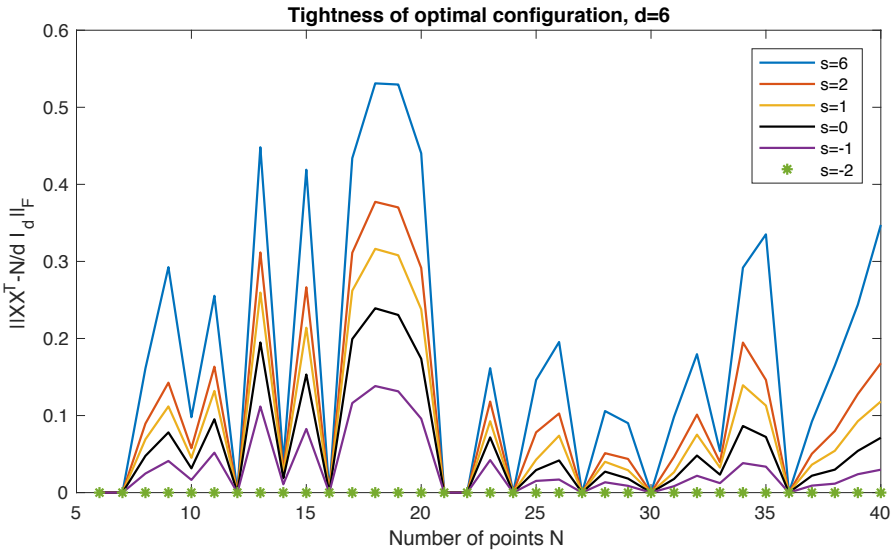

FIGURE 4. Tightness for $d = 6$.

recall that every local minimizer is a global minimizer; i.e., a tight frame [4]. The output of `fminunc` is certainly affected by the initial input. As seen in Figure 1 and Figure 2, the tight frames found by minimizing the frame potential using random initializations generically have poor separation. We propose the following approach for generating well-separated tight frames in $\mathcal{S}(d, N)$ for given d and N.

(1) Generate a random frame $X \in \mathcal{S}(d, N)$.
(2) Using X as an initial configuration, use an optimization algorithm (such as gradient descent) to find a local minimizer Y for (1.10) for some $s > d - 1$. Motivated by Theorems 6.3 and 6.4 the minimizer Y is expected to be well-separated and nearly tight.
(3) Minimize (1.13) with $s = -2$ using Y as the initial configuration. The experiments presented below suggest that the resulting frame is well-separated and tight.

Variations on this approach such as iterating steps 2 and 3 or minimizing Riesz-s energy restricted to the manifold of tight frames will be explored in future work.

Figure 5 shows the performance of the optimal configuration of minimizing frame potential with the initialization being the optimal configuration obtained through solving (1.10). The numerics indicate that these optimal tight configurations are indeed well-separated. The left graph of Figure 5 should be compared to Figure 2 (the values of s used in step 2 of the above algorithm are indicated in the figure and include values of $s < d - 1$). Numerically, this is a promising way to find well-separated tight frames, which has many applications including signal transmission [44, 52].

The set of finite unit norm frames is topologicaly connected, and an irreducible variety [19], but our experiment suggests that for a local minima of (1.10), there will be a tight frame close to it. This can perhaps be explained by the recently solved

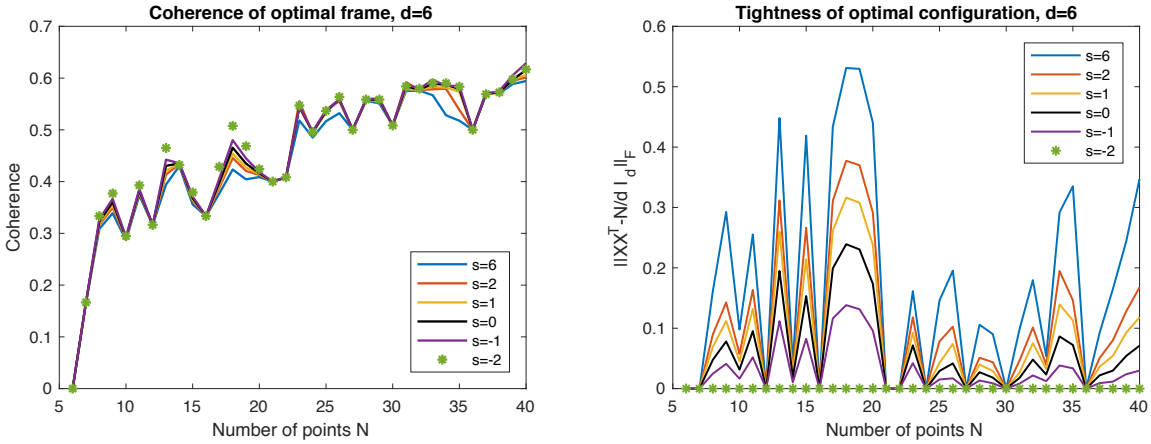

FIGURE 5. The optimal configuration for $s = -2$ with for various choice of s used in step 2 for initialization.

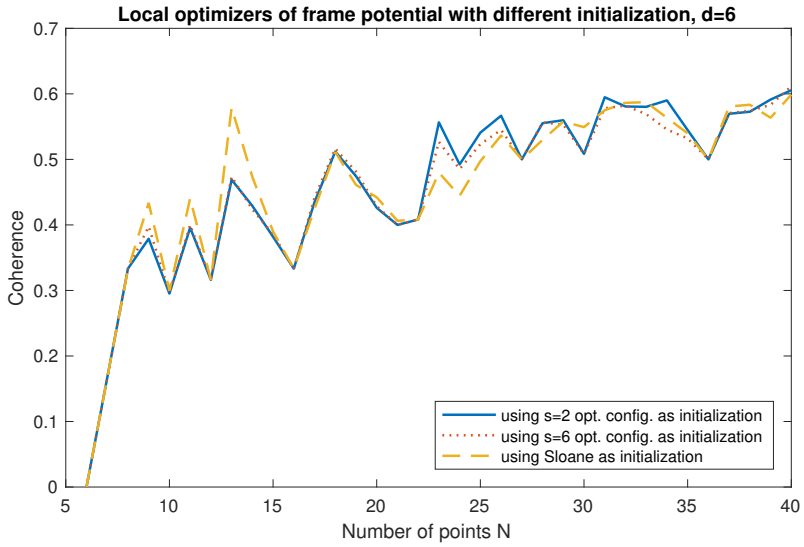

FIGURE 6. Separation comparison of minimizing frame potential with different initializations

Paulsen Problem [47], which implies that for a nearly tight unit norm frame F, there exists a unit norm tight frame nearby since we have shown that a local minima of (1.10) is nearly tight. This suggests that step 3 will result in a nearby tight configuration if the configuration from step 2 is nearly tight as indicated in Theorem 6.4 for N large.

To further see how the initializations impact the frame potential problem, Figure 6 compares the coherence of the optimal configuration of solving (1.13) ($s = -2$) with different initializations. The results are similar, but note that starting with Sloane points, the best separated points among the three, does not necessarily end up with the best separation.

Appendix A

A.1. **Uniform measure.** Given the hypersphere $\mathbb{S}^{d-1}$, let $C_r(x)$ be the hyperspherical cap centered at x, with r being the Euclidean distance of the furthest point to x. That is,

$$C_r(x) = \{y \in \mathbb{S}^{d-1} : \|x - y\| \leq r\}.$$

Recalling that σ_{d-1} denotes the normalized surface measure, the following asymptotic formula holds:

$$\sigma_{d-1}(C_r(x)) = \frac{1}{d-1}\gamma_d r^{d-1} + \mathcal{O}(r^{d+1}), \qquad (r \to 0), \tag{A.1}$$

and also the estimate

$$\sigma_{d-1}(C_r(x)) \leq \frac{1}{d-1}\gamma_d r^{d-1}, \tag{A.2}$$

where

$$\gamma_d := \frac{\Gamma(d/2)}{\Gamma((d-1)/2)\Gamma(1/2)}. \tag{A.3}$$

Both estimates can be found in Section 3 of [54].

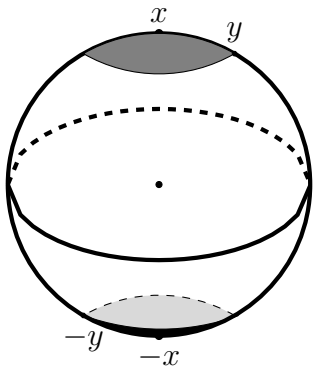

Figure 7. $F^{-1}(B(p_x, r))$

Lemma A.1. *When $\mathbb{H} = \mathbb{R}$, the uniform measure on $\mathcal{D}$ is $(d-1)$-regular. Moreover, we have the estimate*

$$\Phi(\sigma_{d-1})(B(p_x, r)) \leq \frac{2}{d-1}\gamma_d r^{d-1}, \quad \text{for any } p_x \in \mathcal{D}, 0 < r \leq \text{diam}(\mathcal{D}) \tag{A.4}$$

Proof. $\mathcal{D}$ is the projective space embeded in $\mathbb{RM}^h_{d\times d}$. p_x and p_y are furthest away if $x \perp y$, so $\text{diam}(\mathcal{D}) = \sqrt{2}$.

For any point $p_x = F(x) \in \mathcal{D}$ and any $r \leq \text{diam}(\mathcal{D}) = \sqrt{2}$, suppose in the set $B(p_x, r) \cap \mathcal{D}$, p_y is the point that is furthest away from p_x. We can pick y so that $\langle x, y\rangle \geq 0$. Then $\Phi^{-1}(B(p_x, r))$ is the union of the spherical cap centered at x with boundary point y together with its antipodal image, see Figure 7. By (3.3),

$$|\langle x, y\rangle|^2 = 1 - \|p_x - p_y\|^2/2 \geq 1 - r^2/2,$$

$$||x-y||^2 = 2 - 2\langle x, y\rangle \leq 2 - 2\sqrt{1-r^2/2} \leq 2 - 2(1-r^2/2) = r^2.$$

By (A.2),

$$\Phi(\sigma_{d-1})(B(p_x, r)) = \sigma_{d-1}(\Phi^{-1}(B(x,r))) = 2\sigma_{d-1}(C_r(x)) \leq \frac{2}{d-1}\gamma_d r^{d-1}.$$

□

A.2. **Expected value of coherence.** Let $X = \{x_i\} \in \mathcal{S}(d, N)$ be a random configuration on the sphere where each point is selected from a uniform distribution on the sphere. Let $\Theta = \min_{i\neq j} \arccos\langle x_i, x_j\rangle$, so

$$\xi(X) = \max_{i\neq j} |\langle x_i, x_j\rangle| \geq \max_{i\neq j} \langle x_i, x_j\rangle = \cos\Theta \geq 1 - \Theta^2/2. \tag{A.5}$$

It is proven in [20, Theorem 2] that $F_N(t) := \Pr(N^{2/(d-1)}\Theta \leq t) \to F(t)$ where $F(t) = 1 - \exp(-\frac{\gamma_d}{2(d-1)}t^{d-1})$ is supported on $(0, \infty)$.

In order to compute the expected value of Θ^2, we define $G_N(s) := \Pr(N^{4/(d-1)}\Theta^2 \leq s) = F_N(\sqrt{s}) \to F(\sqrt{s})$. By a similar argument as the one in [17, Corollary 3.4], we get

$$\begin{aligned}\lim_{N\to\infty} \mathbb{E}(N^{4/(d-1)}\Theta^2) &= \lim_{N\to\infty} \int_0^\infty (1 - G_N(s))ds \\ &= \int_0^\infty 1 - F(\sqrt{s})ds = \int_0^\infty \exp(-\frac{1}{2}\kappa_d s^{\frac{d-1}{2}}) := C_d\end{aligned}$$

By (A.5), we have

$$\mathbb{E}(\xi(X)) \geq \mathbb{E}(1 - \Theta^2/2) \sim 1 - \frac{C_d}{2}N^{-\frac{4}{d-1}}.$$

References

1. B. Alexeev, J. Cahill, and D. G. Mixon. *Full spark frames.* J. Fourier Anal. Appl. 18.6 (2012): 1167-1194.
2. R. Balan, P. Casazza, and D. Edidin. *On signal reconstruction without phase.* Appl. Comput. Harmon. Anal. 20.3 (2006): 345-356.
3. F. Bachoc, M. Ehler, and M. Gräf. *Optimal configurations of lines and a statistical application.* Adv. Comput. Math. 43.1 (2017): 113-126.
4. J. Benedetto and M. Fickus. *Finite normalized tight frames.* Adv. Comput. Math. 18.2-4 (2003): 357-385.
5. J. Benedetto and J. D. Kolesar. *Geometric properties of Grassmannian frames for $\mathbb{R}^2$ and $\mathbb{R}^3$.* EURASIP J on Adv. in Signal Process. 2006.1 (2006): 049850.
6. D. Bilyk, A. Glazyrin, R. Matzke, J. Park, and O. Vlasiuk. *Optimal measures for p-frame energies on spheres.* arXiv preprint arXiv:1908.00885 (2019).
7. L. Bétermin and E. Sandier, *Renormalized energy and asymptotic expansion of optimal logarithmic energy on the sphere.* Constr. Approx. 47.1 (2018): 39-74.
8. G. Björck. *Distributions of positive mass, which maximize a certain generalized energy integral.* Ark. Mat. 3.3 (1956): 255-269.
9. T. Blumensath and M. E. Davies. *Iterative hard thresholding for compressed sensing.* Appl. Comput. Harmon. Anal. 27.3 (2009): 265-274.

10. B.G. Bodmann and J. I. Haas. *Frame potentials and the geometry of frames.* J. Fourier Anal. Appl. (2014): 1-40.
11. B.G. Bodmann and J. I. Haas. *Low frame coherence via zero-mean tensor embeddings.* Wavelets and Sparsity XVII. Vol. 10394. Internat. Soc. for Optics and Photonics, 2017.
12. A.V. Bondarenko, D.P. Hardin, and E.B. Saff. *Mesh ratios for best-packing and limits of minimal energy configurations.* Acta Math. Hungar. 142.1 (2014): 118-131.
13. S.V. Borodachov, D.P. Hardin, and E.B. Saff. *Asymptotics for discrete weighted minimal Riesz energy problems on rectifiable sets.* Trans. Amer. Math. Soc. 360.3 (2008): 1559-1580.
14. S.V. Borodachov, D.P. Hardin, and E.B. Saff. *Discrete Energy on Rectifiable Sets*, Springer, New York. 2019.
15. J. Bourgain, S. J. Dilworth, K. Ford, S. V. Konyagin, and D. Kutzarova. *Breaking the k^2 barrier for explicit RIP matrices.* Proc. of the forty-third annual ACM Symp. on Theory of computing. ACM, 2011.
16. P. Boyvalenkov, P. Dragnev, D.P. Hardin, E.B. Saff, and M. Stoyanova *Energy Bounds for Codes in Polynomial Metric Spaces*, Anal. Math. Phys., 9.2, (2019): 781-808,
17. J. S. Brauchart, A. B. Reznikov, E. B. Saff, I. H. Sloan, Y. G. Wang, and R. S. Womersley. *Random point sets on the sphere – hole radii, covering, and separation.* Exp. Math. 27.1 (2018): 62-81.
18. J. S. Brauchart, E. B. Saff, I.H. Sloan, and R.S. Womersley. *QMC designs: optimal order Quasi Monte Carlo integration schemes on the sphere.* Math. Comp. 83.290 (2014): 2821-2851.
19. J. Cahill, D. G. Mixon, and N. Strawn. *Connectivity and irreducibility of algebraic varieties of finite unit norm tight frames.* SIAM J. Appl. Algebra Geom. 1.1 (2017): 38-72.
20. T. Cai, J. Fan, and T. Jiang. *Distributions of angles in random packing on spheres.* J. Mach. Learn. Res. 14.1 (2013): 1837-1864.
21. E. Candes, Y. C. Eldar, D. Needell, and P. Randall. *Compressed sensing with coherent and redundant dictionaries.* Appl. Comput. Harmon. Anal. 31.1 (2011): 59-73.
22. E. Candes, T. Strohmer, and V. Voroninski. *Phaselift: Exact and stable signal recovery from magnitude measurements via convex programming.* Commun. Pure Appl. Math. 66.8 (2013): 1241-1274.
23. P. G. Casazza, J. Cahill, J. I. Haas, and J. Tremain. *Constructions of biangular tight frames and their relationships with equiangular tight frames.* arXiv preprint arXiv:1703.01786 (2017).
24. X. Chen, V. Gonzalez, E. Goodman, S. Kang, and K. Okoudjou. *Universal optimal configurations for the p-frame potentials.* Adv. Comput. Math. 46.4 (2020)
25. X. Chen, G. Kutyniok, K. Okoudjou, F. Philipp, and, R. Wang. *Measures of scalability*, IEEE Trans. Inform. Theory, 8(2015): 4410-4423.
26. X. Chen and A. M. Powell. *Almost sure convergence of the Kaczmarz algorithm with random measurements.* J. Fourier Anal. and Appl. 18.6 (2012): 1195-1214.
27. X. Chen and A. M. Powell, *Random subspace actions and fusion frames*, Constr. Approx. 43.1 (2016): 103-134.
28. X. Chen, H. Wang, and R. Wang. *A null space analysis of the ℓ_1-synthesis method in dictionary-based compressed sensing* Appl. and Comput. Harmon. Anal. 37.3 (2014): 492-515.
29. G. Choquet. *Diametre transfini et comparaison de diverses capacités.* Séminaire Brelot-Choquet-Deny. Théorie du potentiel 3.4 (1958): 1-7.
30. H. Cohn and A. Kumar. *Universally optimal distribution of points on spheres.* J. Amer. Math. Soc. 20.1 (2007): 99-148.
31. H. Cohn, A. Kumar, and G. Minton, *Optimal simplices and codes in projective spaces*, Geometry & Topology 20.3 (2016), 1289-1357
32. J. H. Conway, R. H. Hardin, and N. J. A. Sloane. *Packing lines, planes, etc.: Packings in Grassmannian spaces.* Exp. Math. 5.2 (1996): 139-159.
33. L. Dai, M. Soltanalian, and K. Pelckmans. *On the Randomized Kaczmarz Algorithm*, IEEE Signal Process. Lett., 21(3), 330-333, 2014.

34. I. Daubechies, A. Grossmann, and Y. Meyer. *Painless nonorthogonal expansions.* J. Math. Phys. 27.5 (1986): 1271-1283.
35. P. Delsarte, J. M. Goethals, and J. J. Seidel. *Bounds for systems of lines, and Jacobi polynomials.* Geom. and Comb. 1991. 193-207.
36. R. J. Duffin and A. C. Schaeffer. *A class of nonharmonic Fourier series*, Trans. Amer. Math. Soc. 72 (2): 341-366, 1952.
37. M. Ehler. *Random tight frames.* J. Fourier Anal. and Appl 18.1 (2012): 1-20.
38. M. Ehler and K. Okoudjou. *Minimization of the Probabilistic p-frame Potential*, J. Statist. Plann. Inference, 142 (2012), no. 3, 645-659.
39. B. Farkas and B. Nagy. *Transfinite diameter, Chebyshev constant and energy on locally compact spaces.* Potential Anal. 28.3 (2008): 241-260.
40. L. Fejes Tóth, L. *On the sum of distances determined by a pointset.* Acta Math. Hungar. 7.3-4 (1956): 397-401.
41. M. Fickus, J. Jasper, and D. G. Mixon. *Packings in real projective spaces.* SIAM J on Appl. Algebra and Geom. 2.3 (2018): 377-409.
42. M. Fickus and D. G. Mixon. *Tables of the existence of equiangular tight frames.* arXiv preprint arXiv:1504.00253 (2015).
43. S. Foucart. *Flavors of compressive sensing.* Internat. Conf. Approx. Theory. Springer, Cham, 2016.
44. V. K. Goyal, J. Kovačević, and J. A. Kelner. *Quantized frame expansions with erasures.* Appl. and Comput. Harmon, Anal. 10.3 (2001): 203-233.
45. D. Gross, F. Krahmer, and R. Kueng. *A partial derandomization of phaselift using spherical designs.* J. Fourier Anal. Appl. 21.2 (2015): 229-266.
46. J. I. Haas, N. Hammen, and D. G. Mixon. *The Levenstein bound for packings in projective spaces.* Wavelets and Sparsity XVII. Vol. 10394. Internat. Soc. for Optics and Photonics, 2017.
47. L. Hamilton and A. Moitra. *The Paulsen Problem Made Simple.* Proceedings of the 10th Annual Innovations in Theoretical Computer Science (ITCS 2019)
48. D.P. Hardin, T. Leblé, E.B. Saff, and S. Serfaty. *Large deviation principles for hypersingular Riesz gases.* Constr. Approx. 48.1 (2018): 61-100.
49. D. P. Hardin and E. B. Saff. *Minimal Riesz energy point configurations for rectifiable d-dimensional manifolds.* Adv. Math. 193.1 (2005): 174-204.
50. D. P. Hardin, E. B. Saff, and J. T. Whitehouse. *Quasi-uniformity of minimal weighted energy points on compact metric spaces.* J. Complexity 28.2 (2012): 177-191.
51. R. W. Heath, T. Strohmer, and A. J. Paulraj. *On quasi-orthogonal signatures for CDMA systems.* IEEE Trans. on Inform. Theory 52.3 (2006): 1217-1226.
52. R. B. Holmes and V. I. Paulsen. *Optimal frames for erasures.* Linear Algebra Appl. 377 (2004): 31-51.
53. F. Krahmer, D. Needell, and R. Ward. *Compressive sensing with redundant dictionaries and structured measurements.* SIAM J. Math. Anal. 47 (2015), no. 6: 4606–4629.
54. A. B. J. Kuijlaars and E. B. Saff. *Asymptotics for minimal discrete energy on the sphere.* Trans. Amer. Math. Soc. 350.2 (1998): 523-538.
55. A. B. J. Kuijlaars, E. B. Saff, and X. Sun. *On separation of minimal Riesz energy points on spheres in Euclidean spaces.* J. Comput. Appl. Math. 199.1 (2007): 172-180.
56. N. S. Landkof. *Foundations of modern potential theory.* Springer, New York, 1972.
57. J. M. Lee, *Introduction to Smooth Manifolds.* Springer, New York, NY, 2003. 1-29.
58. V. I. Levenshtein, *Designs as maximum codes in polynomial metric spaces.* Acta Appl. Math. 29.1-2 (1992): 1-82.
59. S. Li. *Concise formulas for the area and volume of a hyperspherical cap.* Asian J. Math. and Stat. 4.1 (2011): 66-70.
60. P. Mattila. *Geometry of sets and measures in Euclidean spaces: fractals and rectifiability.* Vol. 44. Cambridge University Press, 1999.

61. R. E. Schwartz. *Five Point Energy Minimization: A Synopsis.* Constr. Approx. 51 (2020): 537–564.
62. Z. Shen. *Wavelet frames and image restorations.* Proc. of the Internat. Congr. of Mathematicians 2010 (ICM 2010) (In 4 Volumes) Vol. I: Plenary Lectures and Ceremonies Vols. II-IV: Invited Lectures. 2010.
63. T. Strohmer and R. W. Heath Jr. *Grassmannian frames with applications to coding and communication.* Appl. Comput. Harmon. Anal. 14.3 (2003): 257-275.
64. T. Strohmer and R. Vershynin. *A randomized Kaczmarz algorithm with exponential convergence.* J. Fourier Anal. Appl. 15 (2009), no. 2, 262–278.
65. M. A. Sustik, J. A. Tropp, I. S. Dhillon, and R. W. Heath Jr. *On the existence of equiangular tight frames.* Linear Algebra Appl. 426.2-3 (2007): 619-635.
66. J. A. Tropp. *Greed is good: Algorithmic results for sparse approximation.* IEEE Trans. Inform. Theory 50.10 (2004): 2231-2242.
67. E. V. Tsiligianni, L. P. Kondi, and A. K. Katsaggelos. *Construction of incoherent unit norm tight frames with application to compressed sensing.* IEEE Trans. Inform. Theory 60.4 (2014): 2319-2330.
68. L. Welch. *Lower bounds on the maximum cross correlation of signals (Corresp.).* IEEE Trans. Inform. Theory 20.3 (1974): 397-399.
69. W. K. Wootters and B. D. Fields. *Optimal state-determination by mutually unbiased measurements.* Ann. Physics 191.2 (1989): 363-381.
70. Z. Zhou, C. Ding, and N. Li. *New families of codebooks achieving the Levenstein bound.* IEEE Trans. Inform. Theory 60.11 (2014): 7382-7387.

Department of Mathematics and Statistics, University of North Carolina Wilmington

E-mail address: chenxuemei@uncw.edu

Center for Constructive Approximation, Department of Mathematics, Vanderbilt University, Nashville, Tennessee 37240

E-mail address: doug.hardin@Vanderbilt.Edu

Center for Constructive Approximation, Department of Mathematics, Vanderbilt University, Nashville, Tennessee 37240

E-mail address: edward.b.saff@vanderbilt.edu